Biogeochemistry (2024) 167:1589–1607
https://doi.org/10.1007/s10533-024-01188-2

High spatial variability in wetland methane fluxes is tied to vegetation patch types

Graham A. Stewart · Sean J. Sharp · Aileen K. Taylor · Michael R. Williams · Margaret A. Palmer

Received: 24 June 2024 / Accepted: 11 October 2024 / Published online: 26 October 2024

Abstract Wetlands are the largest natural source of methane (CH_4), but spatial variability in fluxes complicates prediction, budgeting, and mitigation efforts. Despite the many environmental factors identified as CH_4 drivers, the overall influence of wetland spatial heterogeneity on CH_4 fluxes remains unclear. We identified five dominant patch types—submersed aquatic vegetation (SAV), emergent forbs, sedges/rushes, grasses, and open water—within a freshwater wetland in Maryland, USA, and measured CH_4 fluxes using a combined chamber and eddy covariance approach from June to September 2021. Because patch types integrate co-occurring environmental factors, we hypothesized that CH_4 flux is best characterized at the patch scale. Chamber measurements from representative patches showed distinct CH_4 signals; fluxes from grasses and sedges/rushes were highest, while fluxes from SAV and forbs were lower but skewed, suggesting episodic emission pulses. Open water had the lowest fluxes. Differences between patches were consistent over time, and spatial variability was greater between patches than within them, highlighting patches as key drivers of flux variability. By combining chamber fluxes with eddy covariance data in a Bayesian framework, we provide evidence that patch-type fluxes scale over space and time. Understanding spatial heterogeneity is essential for quantifying wetland contributions to global biogeochemical cycles and predicting the impacts of environmental change on wetland ecosystem processes. Our study demonstrates the importance of vegetation patch types in structuring spatial variability and supports a patch-explicit representation to reduce uncertainty in wetland CH_4 fluxes.

Keywords Freshwater wetland · Greenhouse gas emissions · Spatial heterogeneity · Vegetation type · Chamber method · Eddy covariance

Responsible Editor: Scott Neubauer.

Supplementary Information The online version contains supplementary material available at https://doi.org/10.1007/s10533-024-01188-2.

G. A. Stewart (✉) · S. J. Sharp · A. K. Taylor · M. R. Williams · M. A. Palmer
Department of Entomology, University of Maryland, 4112 Plant Sciences Building, College Park, MD, USA
e-mail: grahamstewart12@gmail.com

M. A. Palmer
National Socio-Environmental Synthesis Center, University of Maryland, 4112 Plant Sciences Building, College Park, MD, USA

Introduction

Wetlands are hotspots of biogeochemical activity and are characterized by spatially variable processes (McClain et al. 2003; Capps et al. 2014; Marton et al. 2015). Methane (CH_4) flux, in particular, is highly scrutinized in wetlands because of its

potency as a greenhouse gas (Whiting and Chanton 2001). Most wetlands contain sufficient organic carbon (C) substrate, reducing conditions, and methanogenic archaea to produce CH_4 (Bridgham et al. 2013), but fluxes within wetlands can exhibit extreme spatial variability (Yavitt et al. 2018). As a result, scaling up flux measurements is an acute challenge (McNicol et al. 2023), and wetlands are a major source of uncertainty in the global CH_4 budget (Bousquet et al. 2006). Alongside efforts to identify spatial drivers of variability (e.g., Girkin et al. 2019; Praetzel et al. 2021), a comprehensive framework is required to understand the relationship between environmental heterogeneity and CH_4 flux.

In many wetlands, spatial heterogeneity is organized into discrete patch types (Marani et al. 2006). Wetlands are often described as patterned mosaics (e.g., Matthes et al. 2014; Morin et al. 2017), with patches distinguished by physical features like microtopography and plant community (Lampela et al. 2016; Keshta et al. 2023). The mechanisms of patch formation vary but are thought to involve self-reinforcing feedback among plants, soil, and hydrological regimes. Through this process, local conditions that initially favor a particular plant assemblage can become increasingly distinct as the plants modify their environment, leading to persistent patches (Marani et al. 2006). In addition to their ecological importance, patches are an accessible means of describing spatial heterogeneity because they can be detected visually and with remote sensing (Dronova et al. 2011).

Wetland vegetation patches integrate co-occurring drivers of spatial variability in CH_4 flux (Davidson et al. 2016). Spatial heterogeneity in abiotic factors, such as flooding regime and soil nutrients, regulates the distribution of wetland vegetation (Day et al. 1988); thus, patch types represent the physicochemical conditions that favor their dominant plants (Couwenberg et al. 2011). Over time, positive feedbacks may further differentiate patches. Plant inputs modify soil chemistry (Palozzi and Lindo 2017), and some wetland plants engineer their physical environment to favor their own dominance (Caraco et al. 2006), resulting in stronger aboveground-belowground linkages and additional spatial variation (Jones et al. 1994). Altogether, the interactions between plants and the abiotic environment shape microbial communities (Berg and Smalla 2009), providing the basis for CH_4 variability among patch types (Sharp et al. 2024).

Plants directly influence patch CH_4 fluxes through physiological mechanisms. The release of oxygen and root exudates into the rhizosphere affects rates of CH_4 production and oxidation, and in emergent plants with porous aerenchyma tissue, vascular gas transport can be an efficient pathway for CH_4 emission (Laanbroek 2010; Vroom et al. 2022). These processes are mediated by species-specific traits, such as internal conductance and the chemical composition of root exudates (Girkin et al. 2018; Villa et al. 2020). Plants may also regulate CH_4 fluxes through microbial community composition, for example, by favoring certain groups of soil methanogens (Waldo et al. 2022; Sharp et al. 2024) or supporting epiphytic methanotrophs (Yoshida et al. 2014). A plant's net effect on flux is thus determined by its impact on multiple interacting—and often competing—processes (Noyce and Megonigal 2021; Bastviken et al. 2023). Plant functional groups and traits can partially explain interspecific variability (Kao-Kniffin et al. 2010; Sutton-Grier and Megonigal 2011), but accuracy depends on how groups are classified and which traits are measured (Gray et al. 2013; Laine et al. 2022).

Variation in CH_4 drivers may lead to different temporal flux dynamics between vegetation patches. Patch structure may determine the dominant emission pathway; for example, in one study plant-mediated transport accounted for the most flux in emergent vegetation, whereas ebullition (i.e., bubbling) was more important in deep water with floating vegetation (Desrosiers et al. 2022). Patch types may also respond differently to environmental fluctuations or long-term changes, modulating patch effects on fluxes (Whitaker et al. 2021; Noyce and Megonigal 2021). In vegetated patches, recent studies have suggested that plant phenology is a strong driver of seasonal flux patterns (Helfter et al. 2022; Ge et al. 2023).

Here, we investigated the link between vegetation patches and CH_4 flux in a spatially heterogeneous wetland. Vegetation patches, as "environmental integrators" of CH_4 drivers, may be most effective at explaining spatial patterns in CH_4 fluxes (Davidson et al. 2016). Further understanding how vegetation patches influence spatially variable processes is essential for estimating the contributions of wetlands to global biogeochemical cycles amid widespread environmental change in these systems. Specifically,

we asked: (1) How do fluxes vary among different vegetation patches? (2) How does variability among patches compare with other sources of spatial and temporal variability? and (3) Can patch-type fluxes be estimated at the wetland scale?

Methods

Site description and patch types

We conducted our study in a wetland within the Choptank River watershed on the Mid-Atlantic Delmarva Peninsula (Caroline County, MD, USA). The climate is humid subtropical, with an annual mean temperature of 13.3 °C and precipitation of 1210 mm distributed evenly across months (30-year normal, 1991–2020; PRISM climate mapping system). Nontidal wetlands in this region are freshwater mineral-soil depressions, with seasonal hydrology characterized by inundation for most of the year with a period of evapotranspiration-driven water table drawdown from late summer to autumn (Phillips and Shedlock 1993). The study wetland (2.08 ha) was briefly drained and used as a pasture in the 1980s, and was ecologically restored in 2003 by plugging drainage ditches, felling encroaching woody vegetation, and removing nonnative plants (Spadafora et al. 2016).

Patch types were selected based on their prevalence in the study wetland, importance in wetlands throughout the region, and representation of plant growth forms (Schultz and Pett 2018; Table 1). Unvegetated open water appeared only in the deepest central part of the wetland. Submersed aquatic vegetation (SAV), such as rooted *Juncus repens* or *Proserpinaca palustris*, formed dense mats in deep areas surrounding open water. Emergent forbs, mainly *Persicaria hydropiperoides*, occupied interstitial spaces between graminoid patches or shallow water near the forested margin of the wetland. We divided graminoid vegetation into two types: grass patches dominated by *Panicum hemitomon* and sedge/rush patches with multiple dominant species (e.g., *Carex striata*), which often grow together. Grasses formed dense monospecific stands underlain by mats of semi-decomposed litter, while sedges/rushes (henceforth "sedges") clustered in tussocks and occupied shallower areas toward the wetland margin. These distinctions are commonly used in wetland studies to represent plant morphological differences (e.g., De Steven et al. 2006; Johns et al. 2015), and may be associated with functional differences (Pan et al. 2020; Williams et al. 2020).

Patch vegetation parameters

Aboveground plant biomass and leaf area index were measured to quantify physical differences in patch vegetation. We chose these parameters because they are easily measured, detectable with remote sensing, and linked to spatial variability in plant productivity and CH_4 flux (Goud et al. 2017, 2022; Villa et al. 2020). In late September, during the late growing season, we sampled vegetation from 0.25 m^2 quadrats in emergent patch types (forbs, sedges, and grasses; n = 3 each). Quadrats were positioned away from chamber collars to prevent disturbance in research

Table 1 Description of wetland patch types

Patch type	Dominant plant species	Avg. water depth (m)[a]	Chamber type	Approx. coverage[b]
Submersed aquatic vegetation (SAV)	***Juncus repens***, *Proserpinaca palustris*, *Utricularia sp.*	0.41	Floating	28%
Emergent forbs	***Persicaria hydropiperoides***, *Proserpinaca spp.*, *Ludwigia sphaerocarpa*	0.32	Floating	17%
Sedges/rushes	***Carex striata***, *Juncus effusus*, *Eleocharis quadrangulata*	0.18	Static	35%
Grasses	***Panicum hemitomon***	0.24	Static	10%
Open water	n.a.	0.44	Floating	11%

Plant species in bold were dominant in our study plots. Open water patches had no visible plants. Note that *P. palustris* has both aerial and aquatic growth forms

[a]June–September

[b]Excluding forested area around wetland margin

plots. Plant stems were cut above the soil surface, standing litter was separated, and samples were dried and weighed to determine aboveground biomass (g m^{-2}). To estimate leaf area, we selected ten stems from each quadrat. Leaves were digitally scanned, and area was measured using ImageJ (Schneider et al. 2012) then scaled to the full quadrat by species. Leaf area index (m^2 m^{-2}) was calculated as the total one-sided leaf area in a quadrat, normalized by quadrat area.

To assess the potential role of plant phenology in patch fluxes, we monitored seasonal greenness patterns of the dominant graminoid species. Using a fixed digital camera (StarDot NetCam), we captured a time series of images and defined homogeneous regions of interest (ROIs) for each species. The camera's field of view did not cover emergent forbs and SAV, so our analysis focused on dominant graminoids (Table 1). Following PhenoCam network protocols (Richardson et al. 2018), greenness was calculated for each ROI as the mean pixel green chromatic coordinate (G_{CC}) value, and time series for 2021 were constructed using the 90% cumulative G_{CC} over 3-day windows. Plant active phase was defined as the period when G_{CC} exceeded 10% of its seasonal amplitude (Richardson et al. 2018). This analysis was conducted in R using the *phenopix* and *phenocamr* packages (Filippa et al. 2016; Hufkens et al. 2018).

Flux measurement

We adopted a combined static chamber and eddy covariance (EC) approach to quantify patch-type CH_4 fluxes. The two methods are considered complementary; chambers directly measure fluxes at discrete points, providing high precision but low spatiotemporal coverage, whereas EC offers continuous ecosystem-scale measurements (Morin et al. 2017). Our primary aim was therefore to synthesize rather than contrast their information. Here, we used a Bayesian approach, which allowed us to draw from both chamber and tower data and obtain robust estimates of patch-type fluxes across space and time.

Static chambers

Patch flux point measurements were collected using chamber incubations. We established research plots in one representative of each patch type; plots had three chamber locations approximately 2 m apart (total n = 15 chambers) and were accessed by raised boardwalks to minimize disturbance. We sampled from two types of chambers. In the grasses and sedges, we used static chambers (0.5 × 0.5 × 0.7 m) consisting of aluminum frames covered by clear polycarbonate sheeting, with aluminum lids, to accommodate tall (> 0.5 m) vegetation. In the forbs, SAV, and open water plots we used floating chambers (0.4 × 0.4 × 0.35 m) made from clear acrylic aquaria to avoid inducing mixing in deeper (> 0.3 m) water. Battery-powered fans were placed in the larger static chambers to ensure a well-mixed headspace. For both chamber types, sampling ports were located on top.

Chambers were sampled over a series of three campaigns in the summer of 2021. Campaigns were held in June, July, and September to target the early, peak, and late phases of the growing season, respectively. During each weeklong campaign, we selected three sampling days with similar weather forecasts (see Supplementary Table S1 for more information on sampling conditions). All chambers were sampled each day in full sunlight between 08:00 and 18:00 h and in random order by patch. We conducted an additional sampling day in November but did not include it in the main analysis (data shown in Supplementary Fig. S1). Water depth was monitored continuously with pressure transducers (Onset Computer Corporation, Bourne, MA, USA) in shallow wells at our research plots in each patch type (Supplementary Fig. S2).

Chamber fluxes were measured with 30-min incubations. Gas samples were taken at 10-min intervals (n = 4 per incubation) and stored in 12 mL evacuated vials (Labco, UK). Methane concentrations were determined using gas chromatography (SRI Instruments, Torrance, CA, USA) and corrected with in-chamber temperature measurements. The average temperature change over the course of incubations was 2 °C in static chambers and 3 °C in floating chambers. Fluxes were calculated as the linear rate of change in concentration, accounting for chamber volume and surface area (Holland et al. 1999). Quality control was performed by visual inspection, with the goal of ensuring linearity while retaining as many fluxes as possible. We removed points suspected to be affected by vial leakage, chamber headspace saturation, or excessive disturbance as indicated by deviation from linear trends (7.5% of total points). Flux

curves were retained if at least three points had an $R^2 > 0.9$ (Nahlik and Mitsch 2011) or if the rate was near zero (± 1 mg CH_4-C m^{-2} h^{-1}). We retained near-zero fluxes (including negative fluxes) to avoid biasing our results toward higher fluxes (Repo et al. 2007). Because we took care to minimize effects of disturbance, fluxes with large concentration jumps, presumably due to ebullition, were retained unless they failed our statistical criteria. Out of 150 measured fluxes, 102 were calculated using all four points, 45 had three points, and three were discarded.

Eddy covariance

Continuous wetland-scale CH_4 fluxes were measured using EC (Baldocchi et al. 2001). A 2.9 m tall flux tower located in the open-canopy area of the wetland was equipped with an open-path CH_4 analyzer (LI-7700; LI-COR, Lincoln, NE, USA) and a sonic anemometer (WindMaster Pro; Gill Instruments, UK) to measure turbulent fluctuations. Raw 10 Hz data was processed at 30-min intervals in EddyPro 7.0.9 (LI-COR) using standard methods for sonic anemometer tilt correction, time series detrending, time lag compensation, and statistical screening (Vickers and Mahrt 1997; Wilczak et al. 2001; Moncrieff et al. 2004). Fluxes were corrected for frequency response (Moncrieff et al. 1997, 2004) and air density fluctuations (Webb et al. 1980).

As with chamber measurements, we restricted our analysis to the summer (June–September), which accounted for about 70% of 2021 CH_4 emissions at our site (Supplementary Fig. S3). Fluxes were quality checked using standard tests for stationarity and sufficient turbulence (Foken et al. 2012). We further removed periods during which a plausible time lag was not identified (Eugster et al. 2011), the CH_4 mixing ratio varied excessively (Erkkilä et al. 2018), or the friction velocity was < 0.1 m s^{-1} (Kljun et al. 2015). No gap filling was attempted.

Footprint analysis

Source areas of 30-min tower fluxes were estimated using a two-dimensional analytical footprint model (Kljun et al. 2015). Given the micrometeorological conditions during each flux averaging period, the model applied a source weighting function to assign relative flux contributions to a 1-m grid around the tower (Schmid 1997). All input variables were derived from tower data, except for atmospheric boundary layer height, which was acquired from ERA5 climate reanalysis data (Hersbach et al. 2020). A description of the model including its definition and parameterization can be found in Kljun et al. (2015).

Although explicitly valid for homogeneous land cover, analytical footprint models are commonly used in heterogeneous environments to attribute EC fluxes to spatial features (Neftel et al. 2008). Studies examining flux uncertainty from footprint calculations in such environments have found it to be relatively low (Morin et al. 2017; Stoy et al. 2021); however, we acknowledge that flow inhomogeneities across patch types can introduce error into our footprint estimates (Finnigan 2004). We took several steps to mitigate this bias. Aerodynamic roughness parameters were determined empirically for each flux averaging period to account for the dependence of flow conditions on wind direction (Neftel et al. 2008). Footprints were rejected if excessive roughness concentrated the source area at the tower (peak crosswind-integrated distance < 1 m). We also removed periods with negatively skewed absolute humidity, indicating a potential low-frequency influence on fluxes from outside the footprint area (Esters et al. 2021). Our final dataset included 2605 half-hourly CH_4 fluxes and footprints (2219 day; 386 night).

Flux footprints were superimposed on a patch cover map to determine the relative influence of each patch type on tower flux measurements (Fig. 1). Patch cover was mapped by hand using GPS-referenced field surveys and aerial imagery (0.6 m resolution, color near-infrared; National Agriculture Imagery Program 2021). For each 30-min period, footprint weights were summed by patch type within the tower's source area (Forbrich et al. 2011). Because the footprint model does not define a 100% source area limit, we constrained our analysis to an 80% cumulative footprint and rescaled weights to sum to unity (Chu et al. 2021).

Patch-type flux estimation

To estimate patch-type fluxes at a broader scale, tower flux data was modeled as a simple weighted average:

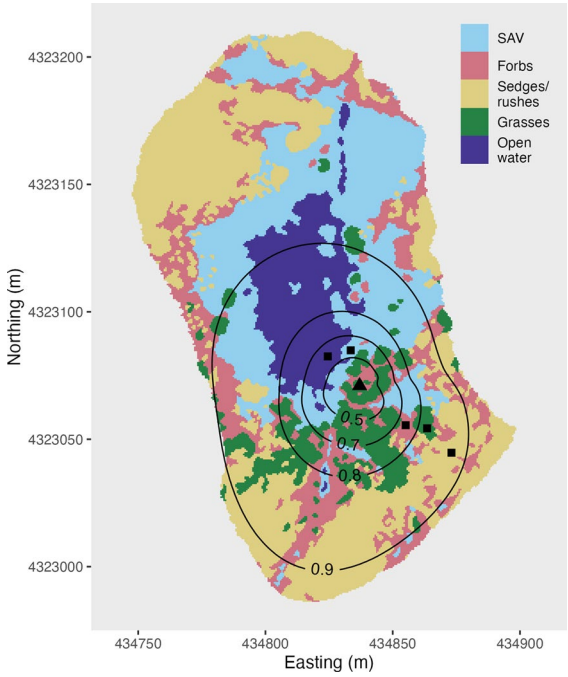

Fig. 1 Distribution of patch types and flux tower source area in the study wetland. The triangular symbol indicates the location of the flux tower. Contour lines refer to the cumulative flux footprint from all half-hourly measurements (n = 2605). All static chambers plots (square symbols) were located within the 90% footprint contour. *SAV* submersed aquatic vegetation

$$F_t = \sum_{i=1}^{n} \overline{f}_i \phi_{it} \quad (1)$$

where F_t is the observed tower flux at time t which integrates a source area composed of n (= 5) patch types, ϕ_{it} is the source area fraction of patch type i at time t (i.e., a patch type's weighted contribution to the tower flux, determined with footprint analysis as detailed above), and $\overline{f}_i$ is the mean flux from patch type i. We excluded an intercept because we assumed that the observed fluxes were influenced only by the defined patch types (Kim et al. 2018). This model is widely used to "disaggregate" fluxes in landscape-scale analyses (e.g., from airborne eddy covariance systems; Hutjes et al. 2010) but less commonly within a single ecosystem. Equation (1) can be made temporally explicit by including environmental response functions in a hierarchical structure (e.g., with soil temperature; Levy et al. 2020); however, because our focus was on estimates of $\overline{f}_i$ (rather than predictions of F_t), we did not add parameters that could complicate the interpretation of $\overline{f}_i$. As such, $\overline{f}_i$ should be considered an estimate of the average flux from a patch type over the study period.

The model was parameterized using Bayesian linear regression. Bayesian methods provide a robust representation of uncertainty and, importantly, allowed us to incorporate prior knowledge on parameter distributions (Ellison 2004). We set normal priors on $\overline{f}_i$:

$$\overline{f}_i \sim \mathcal{N}(\mu_i, \sigma_i) \quad (2)$$

where μ_i and σ_i are the median and median absolute deviation of chamber-measured fluxes from patch type i, respectively. Posterior distributions of $\overline{f}_i$ were estimated iteratively using Markov chain Monte Carlo (MCMC) sampling with tower data. To examine model sensitivity to the chamber prior, we ran a second version using weakly informative priors (i.e., normal distributions with a large spread centered at zero). We also ran the model separately for daytime and nighttime data (Supplementary Fig. S4). Models were evaluated by comparing the observed data distribution with simulated datasets from the posterior predictive distribution (Conn et al. 2018; Supplementary Fig. S5). Models were fit in R using the *rstanarm* package (Goodrich et al. 2020), based on the Stan probabilistic programming language (Carpenter et al. 2017).

A potential concern with the model was multicollinearity among source area fractions, hindering the independent identification of parameters. At our site, source area fractions were correlated because patch types were unevenly distributed around the flux tower (Fig. 1). Although informative priors can mitigate multicollinearity issues in Bayesian analyses (Pesaran and Smith 2019), parameters in our model without the chamber prior likely had some degree of dependence. Parameter identifiability was assessed by examining pairwise correlations between MCMC samples (Ogle and Barber 2020; Supplementary Figs. S6 and S7).

Statistical analysis

Variance in chamber flux data was partitioned into components using a linear random effects model (Harrison et al. 2018). The model included terms for

patch type, chamber (nested within patch type), and sampling campaign. We also evaluated the patch type × campaign interaction. Days were considered replicates because we intentionally selected sampling days with similar weather conditions. The model was fitted with restricted maximum likelihood using the R package *lme4* (Bates et al. 2015). Fluxes were power transformed (Yeo-Johnson) to stabilize variance.

Results

Patch vegetation

Graminoid patch types (sedges and grasses) were most productive according to both aboveground biomass and leaf area index (Table 2). Emergent forbs and SAV had greater leaf area relative to biomass than did graminoids, indicating more allocation of resources to leaf tissue, but aboveground biomass was lower overall in these patches. Sedges had the highest aboveground biomass and leaf area index (361 g m^{-2} and 3.20 m^2 m^{-2}, respectively) and were further characterized by a long growing season (Table 2). Compared with the dominant grass, the dominant sedge in our research plots (*Carex striata*) began green-up earlier, peaked earlier, senesced later, and had a longer active phase (Fig. 2). Phenology also differed between *C. striata* and other dominant sedges/rushes, with all three species exhibiting unique greenness patterns (Fig. 2).

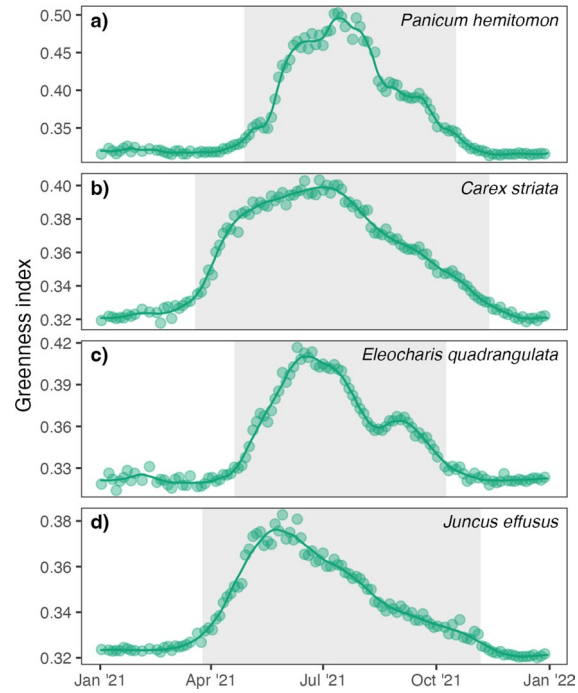

Fig. 2 Species-specific phenology for dominant grasses (**a**) and sedges/rushes (**b–d**) in the study wetland in 2021. Greenness index is the green chromatic coordinate (GCC) derived from digital repeat photography and is shown as smoothed curves on top of 3-day point values. Species are shown on different GCC scales to emphasize individual temporal patterns. Shaded areas denote a plant's active phase, defined as the period when GCC is greater than 10% of its seasonal amplitude

Table 2 Plant productivity in vegetated patches

Patch type	Aboveground biomass, g m^{-2}	Leaf area index, m^2 m^{-2}	Peak greenness, DOY	Active phase length, days
Submersed aquatic vegetation[a]	34.9 (6.9)	0.61 (0.10)	n.r.	n.r.
Emergent forbs	83.6 (15.3)	0.93 (0.18)	n.r.	n.r.
Sedges/rushes[b]	361 (30.9)	3.20 (0.27)	181	239
Grasses	255 (15.8)	2.15 (0.14)	195	172

Biomass and leaf area index are means with standard errors in parentheses (n = 3 quadrats) for live material only, sampled on DOY 259. Peak greenness and active phase were determined by analyzing digital repeat photography as described in section "Patch vegetation parameters". *n.r.* not recorded

[a]Biomass data from Sharp et al. (2024); leaf area estimated using a scaling relationship for *Juncus bulbosus* (morphologically similar to *J. repens*; Jamoneau et al. 2017)

[b]*Carex striata*-dominated patches

Empirical distributions of patch-type fluxes

Chamber flux distributions had distinct shapes among patches (Fig. 3). Most open water fluxes were low (median flux = 0.591 mg CH_4-C m^{-2} h^{-1}); some negative fluxes were observed but were likely below the detection limit. Graminoid patches (grasses and sedges) had the highest median fluxes (16.1, 16.3 mg CH_4-C m^{-2} h^{-1}, respectively) and were positively skewed. Fluxes from SAV and forbs (median = 6.50, 7.09 mg CH_4-C m^{-2} h^{-1}, respectively) were centered between open water and graminoids, spanned almost the full range of fluxes, and had a strong positive skew. The maximum flux was between 32 and 46 mg CH_4-C m^{-2} h^{-1} for all vegetated patches.

Temporal variability in fluxes within patches

Relative differences between patch fluxes were generally consistent over time (Fig. 4). Graminoid (sedge and grass) fluxes were always highest and never fell below 5 mg CH_4-C m^{-2} h^{-1}. Forbs and SAV were most variable among campaigns, but their median fluxes never exceeded those of graminoids. All patch fluxes peaked in July, except for grasses, which decreased with time. Fluxes from forbs and SAV were positively skewed for all campaigns, i.e., these patches had occasional elevated fluxes throughout the summer. Open water fluxes never exceeded 2.2 mg CH_4-C m^{-2} h^{-1} and were always lowest.

Variability among patches was the largest source of chamber flux variability in our study design (Supplementary Table S2). According to our variance component model, *patch* accounted for 65.4% of the variance in power-transformed flux, followed by *chamber* (4.1%) and *campaign* (2.2%). The *patch*×*campaign* interaction had a negligible effect on the model fit and was removed from the analysis. We suspected that low open water fluxes were partially responsible for the large *patch* contribution, so we repeated the analysis with vegetated patches only (Supplementary Table S2). This reduced the *patch* component, but *patch* (19.8%) remained larger than *chamber* (10.8%) and *campaign* (7.0%). In other words, patch variability was greater than temporal variability (among campaigns) and spatial variability within patches. Excluding open water increased the residual unaccounted variance (including among sampling days within *campaign*) from 28.3 to 62.4%.

Summer patch-type fluxes

Over an expanded spatial and temporal inference space, flux tower data supported the patch variability identified with static chambers (Fig. 5). Tower

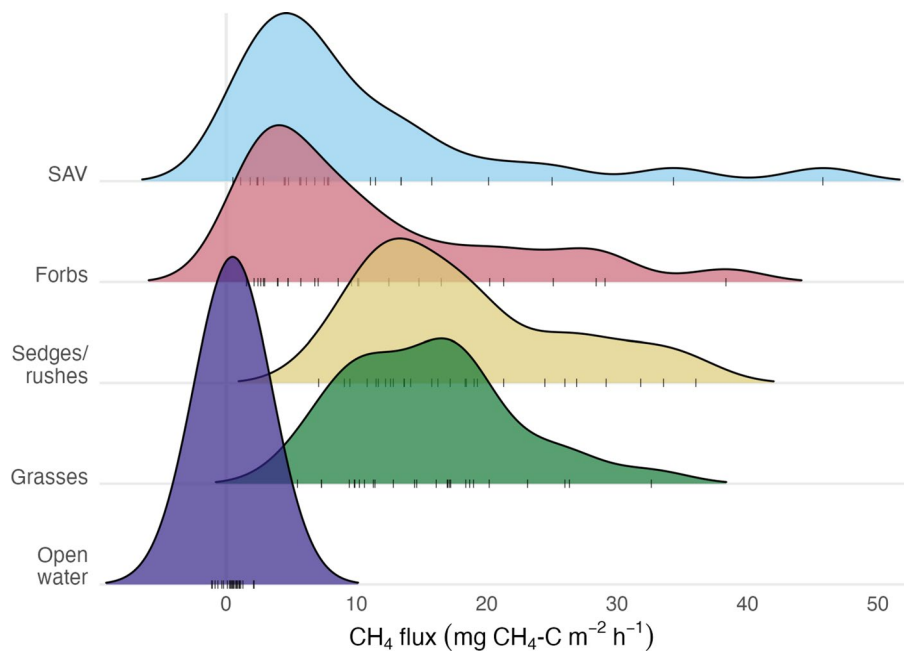

Fig. 3 Patch chamber flux distributions. Individual measurements (n = 25–27 per patch) are shown as tick marks below smoothed density curves. Density was estimated using a joint bandwidth for all patches. *SAV* submersed aquatic vegetation

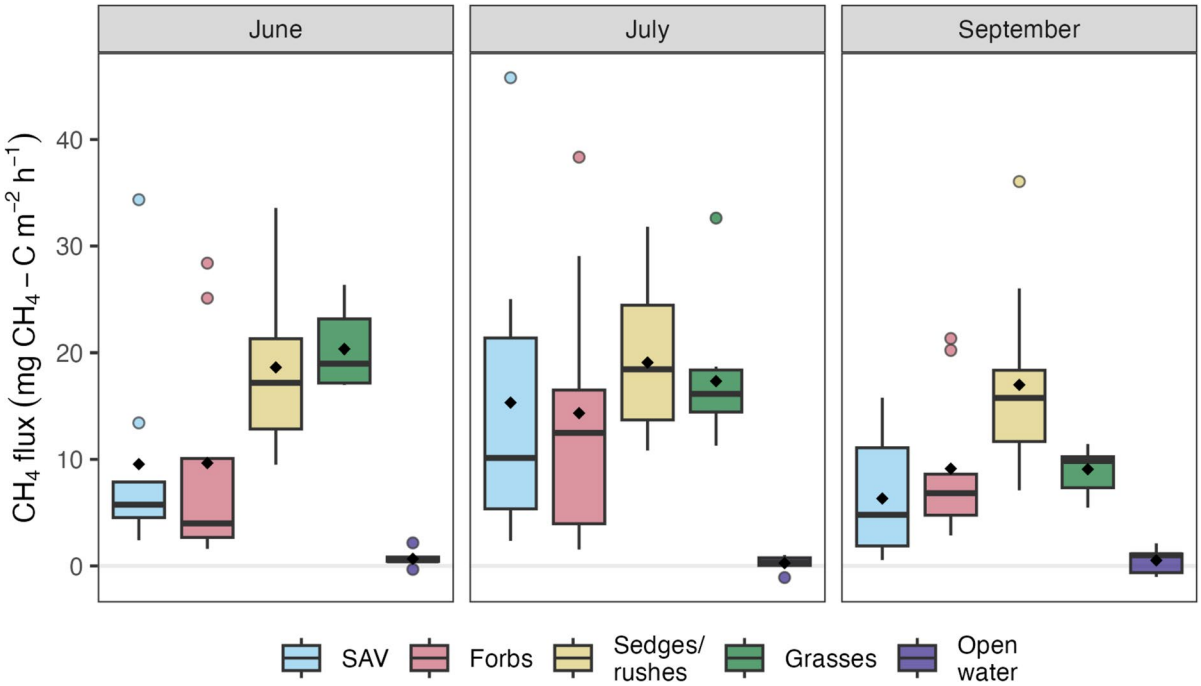

Fig. 4 Patch flux boxplots for the three sampling campaigns. Fluxes (n = 8–9 for each patch per campaign) were measured using chambers in 2021. Campaigns consisted of three sampling days during which three chambers were sampled in each patch. Diamonds are patch-campaign means and colored points lie outside 1.5 times the interquartile range. *SAV* submersed aquatic vegetation

estimates had a similar pattern to chamber data, with highest fluxes from graminoid patches, lowest from open water, and both SAV and emergent forbs falling somewhere in between. Incorporating tower data reduced the uncertainty around mean patch type fluxes, as we expected given the amount of flux tower data relative to chamber measurements. Sedge uncertainty remained relatively high, likely because sedge patches were concentrated furthest from the tower and thus had a small contribution to the flux footprint (Fig. 1; mean source area fraction = 0.6%). Prior distributions specified using chamber data had little effect on patch-type flux estimates; that is, our model produced similar results regardless of whether prior information on patch fluxes was provided. The most notable departure from chamber data was the lower model estimate for grasses. Our model also indicated a small but nonnegligible source of CH_4 from open water, greater than what we measured with floating chambers.

Discussion

Patches have distinct CH_4 flux distributions

Chamber sampling in our wetland revealed that the distribution of CH_4 fluxes had distinct shapes among patch types. This suggests strong spatial variability in the processes driving CH_4 fluxes and supports a patch-specific framework for wetland ecosystem flux. Below, we describe the observed flux distributions and mechanisms that may differentiate them.

Fluxes from sedge and grass (graminoid) patches were consistently highest and had few extremes. Studies across ecoregions and wetland types have shown that graminoid vegetation is a strong source of CH_4 (e.g., Turetsky et al. 2014; Akhtar et al. 2020; Bao et al. 2021). This is partly because dominant graminoids are generally productive, which is considered a driver of wetland CH_4 fluxes (Whiting and Chanton 1993). In our wetland, graminoid productivity was

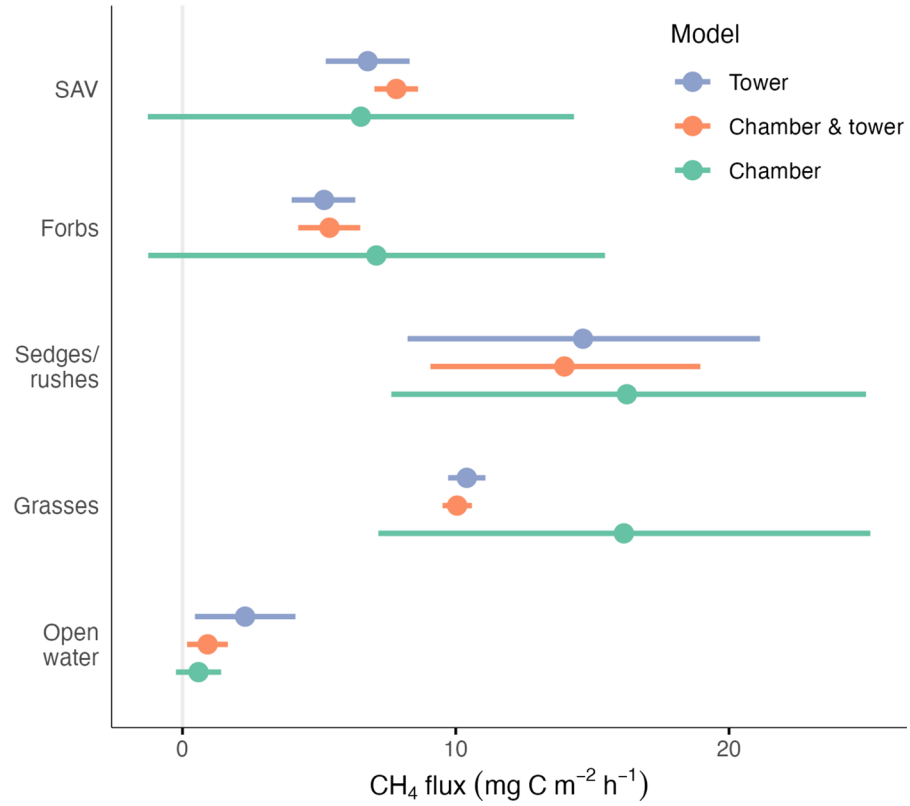

Fig. 5 Estimates of average growing season CH_4 fluxes for wetland patch types from a model using both chamber and tower data ("Chamber & tower" model). The model was a Bayesian linear regression of tower flux on patch source area fraction data, with chamber data as priors on patch flux parameters. Estimates from a model with weakly informative priors ("Tower" model) and from prior probability distributions ("Chamber" model) are also shown. Points and intervals are medians and 80% uncertainty. *SAV* submersed aquatic vegetation

indicated by greater aboveground biomass and leaf area index (Table 2). These traits have been linked to, for example, inputs of litter and root exudates (Sutton-Grier and Megonigal 2011; Goud et al. 2017), which can fuel methanogenesis directly as substrate and indirectly by priming the decomposition of complex soil organic matter into compounds more readily accessible to methanogens (Waldo et al. 2019). We did not measure belowground biomass, which interacts more directly with CH_4-cycling microbes and does not always correlate with aboveground vegetation parameters (Määttä and Malhotra 2024). However, the relationship between biomass and CH_4 fluxes depends on species and abiotic factors (Kao-Kniffin et al. 2010; Bhullar et al. 2013b), indicating that productivity alone is insufficient for explaining plant influences on fluxes.

Plant-mediated transport may also be a factor in high graminoid fluxes. Although all the dominant plants in our wetland develop aerenchyma, graminoid species have highly conductive vascular tissue and extensive root systems, making them effective conduits for CH_4 to the atmosphere (Bhullar et al. 2013a; Ge et al. 2023). The same traits can also increase radial oxygen loss and stimulate CH_4 oxidation (Kao-Kniffin et al. 2010; Sutton-Grier and Megonigal 2011); however, given the high fluxes in graminoid patches, the net effect of these patches on fluxes was evidently positive (McEwing et al. 2015). Along a porewater depth gradient in our study wetland, CH_4 concentrations were reduced in graminoid rooting zones (Sharp et al. 2024), which is characteristic of plant-driven CH_4 transport and rhizosphere oxygenation (van den Berg et al. 2020).

The efficiency of plant-mediated transport can suppress other flux pathways (e.g., ebullition; van den Berg et al. 2020), resulting in a CH_4 signal dominated by plant ventilation. The graminoids in our wetland exchange gases passively, so their influence on CH_4 is likely to be steady rather than, for example, driven by intermittent plant processes (Vroom et al. 2022). Standing litter was abundant in graminoid patches (e.g., 115 g m^{-2} on average in *Carex striata* quadrats; data not shown) and can be an additional passive conduit for CH_4 (Carmichael et al. 2014). Thus, plant-mediated transport may explain the relative

consistency (i.e., few outliers) in our graminoid flux measurements.

Fluxes from emergent forbs and SAV were strongly skewed, indicating that episodic emissions may account for a large proportion of fluxes from these patches. Compared with graminoids, leaf area index of emergent forbs and SAV was lower (Table 2), possibly reflecting less potential surface area for gas exchange and reduced plant-mediated flux (Villa et al. 2020). Root traits such as shallow depth, low surface area, and higher tissue density may also limit vascular gas transport in both emergent forbs and SAV (Andrews et al. 2013; Bhullar et al. 2013a). Nevertheless, C inputs in these patches could support high CH_4 production (Theus et al. 2023), and without an efficient plant conduit, CH_4 can quickly accumulate in the sediment. These conditions promote CH_4 oversaturation and ebullition (Grasset et al. 2019), which could account for episodic fluxes. Others have noted the importance of ebullition in SAV patches (e.g., Jeffrey et al. 2019; Barbosa et al. 2021; but see Villa et al. 2021), and our results highlight that the primary flux pathway may differ between patch types.

Despite being flooded for the length of the study, open water (no vegetation) fluxes remained close to zero. Although we cannot rule out unmeasured pulses, concurrent work in our study wetland revealed high soil porewater CH_4 concentrations beneath open water (Sharp et al. 2024), which could suggest an increased residence time of CH_4 produced in the soil. Open water was found in the deepest areas of our wetland (Table 1), and, without ebullition and plant conduits as efficient transport pathways, most flux likely occurred via slow diffusion. These factors increase the opportunity for CH_4 oxidation by methanotrophs (Rey-Sanchez et al. 2018), and may have moderated open water fluxes in our system.

Patches are an important source of variability in CH_4 flux

Fluxes varied more between than within patches, suggesting that vegetation patchiness is important in explaining spatial heterogeneity in wetland CH_4 flux. Our chambers were placed approximately 2 m apart within patches, so spatial autocorrelation was likely a factor; however, extreme variability has been observed at even shorter distances (Teh et al. 2011; Yavitt et al. 2018). Within vegetated patches, spatial variability in fluxes may be related to local heterogeneity in soils (Briones et al. 2022) or plant density (Theus et al. 2023). Stem counts varied among chambers within our emergent vegetation patches (e.g., coefficient of variation = 38% for grasses; data not shown), but this was not accompanied by a similar degree of flux variability. Thus, differences between patch types appear to outweigh any effects of within-patch biotic and abiotic heterogeneity on CH_4 fluxes.

Variability among summer sampling campaigns was low. Our results follow Turner et al. (2020) and Korrensalo et al. (2022), who observed low intra-seasonal variability in CH_4 fluxes from vegetated patches during the growing season. The relative differences between patches were consistent during the summer and on an additional sampling day in November (Supplementary Fig. S1), suggesting that patches responded similarly to shifts in seasonal conditions. One exception, however, was a decrease in fluxes from grasses relative to sedges (Fig. 4), which may be related to phenological differences. The dominant grass, *Panicum hemitomon*, had a steeper decline in greenness than *Carex striata*, the dominant sedge in our chamber plots (Table 2, Fig. 2). This could result in lower CH_4 fluxes, for example, due to reduced C input to the rhizosphere (Helfter et al. 2022).

Over a full annual cycle, variation in patch plant phenology may be an important determinant of a wetland's annual CH_4 budget. Plant phenology is a functional quality of vegetation patches with respect to CH_4 flux, and temporal dynamics in general should be considered intrinsically linked to spatial heterogeneity in wetlands (Hammond and Kolasa 2014). In our temperate depressional wetland, active phase (indicated by the temporal pattern in greenness) varied among graminoid species and was 67 days longer for the dominant sedge than for the dominant grass (Table 2, Fig. 2). A longer active phase could imply an extended supply of fresh substrate and a prolonged time when aerenchyma tissue is fully developed and can optimally transport gases (Vázquez-Lule and Vargas 2021). Based on this difference, we expect sedges to be a greater per-area CH_4 source relative to grasses than our summer measurements would suggest (Fig. 5).

Patch variability scales over space and time

By incorporating flux tower data, we found that our chamber measurements signified a broader pattern of spatial variability in the study wetland, where CH_4 fluxes varied systematically by patch type. Our results support previous studies suggesting that wetland vegetation patches serve as "environmental integrators", representing distinct arrays of co-occurring CH_4 drivers (Couwenberg et al. 2011; Davidson et al. 2016). Thus, it is likely that wetland-scale CH_4 fluxes depend on patch composition, and efforts to model and inventory wetland CH_4 should account for differences among patch types.

The persistence of a patch signal across a wide range of spatial and temporal variability suggests that CH_4 flux is a functional property of vegetation patches. Our flux tower footprint covered an area of heterogeneous patch composition across a hydrologic gradient within the wetland depression (Fig. 1). Temporally, our data spanned fluctuations in temperature, water level, and other environmental variables within the growing season (Supplementary Figs. S2 and S3). Diel variability was also captured, although to a limited extent as most nighttime fluxes were removed by quality control measures (as is common in EC; Kim et al. 2020). Therefore, it is likely that the patch variability in our wetland is driven by differences in underlying CH_4 dynamics that influence fluxes irrespective of spatial and temporal context.

Unvegetated open water was a minor source of CH_4 in our study. Our model estimate of open water fluxes was higher than chamber measurements alone (Fig. 5), suggesting that chamber sampling may have missed a small but nonnegligible CH_4 source from this patch type. This underscores the need for high-frequency measurements to capture "hot moments" in CH_4 fluxes, which can contribute disproportionately to CH_4 budgets (Anthony and Silver 2021). Nevertheless, open water fluxes were the lowest of the patch types. Flux estimates from our model closely resembled measurements from forested, closed-canopy Delmarva bay wetlands that lacked emergent vegetation (Hondula et al. 2021). This suggests that flux estimates for specific patch types may have broader applicability across landscapes, although literature on this topic is limited. Some previous studies also reported low open water fluxes (e.g., McNicol et al. 2017; Rey-Sanchez et al. 2018), while others found them to be relatively high (e.g., Villa et al. 2021). Further investigation is warranted to determine the factors driving variability in patch-type fluxes among wetlands, and the extent to which patch influence can be generalized across landscapes.

Although the chamber and tower data were remarkably consistent with respect to patch-type fluxes (Fig. 5), there were some differences between the two methods. These results highlight the importance of combining, rather than contrasting, measurements at different scales to interpret wetland fluxes (Morin et al. 2017). Bayesian methods provide an intuitive means of incorporating prior information, and we recommend these methods for studies aiming to reconcile flux measurement approaches.

Tower estimates were generally lower than chamber fluxes (Fig. 5), which is a common finding in studies using both methods (e.g., Krauss et al. 2016; Erkkilä et al. 2018). For emergent forbs, within-type spatial variability may have contributed to this discrepancy. This patch type had multiple dominant species; our forb chambers were placed in a *Persicaria hydropiperoides* patch, but we observed other patches near the flux tower dominated by *Ludwigia sphaerocarpa* and *Proserpinaca* spp. that may have had lower fluxes. Because CH_4 fluxes can vary among species within vegetation types (Ström et al. 2005), we expect within-type variability to increase with the number of dominant species in a wetland. However, mapping wetlands at the species level may be an impractical solution for scaling fluxes and may limit the geographic applicability of flux estimates (Gray et al. 2013). Instead, research should focus on identifying plant or environmental attributes that efficiently distinguish patches based on their CH_4 fluxes (Laine et al. 2022).

Grass fluxes estimated by our tower model were considerably lower than our median chamber measurement (Fig. 5). This difference may reflect unmeasured spatial heterogeneity (e.g., in plant density or soil chemistry), but an alternative explanation is that our intermittent chamber sampling did not adequately capture the temporal dynamics specific to the dominant grass, *Panicum hemitomon*. Between our July and September sampling campaigns, water levels receded below the soil surface in some areas (Supplementary Fig. S2), which may have disproportionately affected CH_4 fluxes from grass patches. *P. hemitomon* grows optimally under flooded conditions

(Holm and Sasser 2008), and we observed a rapid decline in its greenness concurrent with drying, followed by a recovery upon flooding (midway between Jul'21 and Oct'21 in Fig. 2). This response was similarly pronounced for only one of the three dominant sedge/rush species and not for the sedge found in our chamber plot (*Carex striata*; Fig. 2). Hence, grasses may have undergone a disturbance that temporarily reduced their ability to facilitate CH_4 flux and resulted in a lower estimate than our chamber data. This hypothesis could be tested to determine the importance of disturbance events on wetland patch fluxes.

Our study conceptualized a spatially heterogeneous wetland as a mosaic of fixed patch types. Although this framework revealed an important pattern of patch variability, it can be extended in several ways. We suggested that plant phenology may contribute to patch differences, and, in general, overlaying temporal environmental data (e.g., water level, temperature, nutrients) may be necessary to fully understand how fluxes vary among patches (Levy et al. 2020). The spatial distribution of patches is dynamic, especially when wetlands are newly restored, recovering from disturbance, or influenced by external stressors (Taddeo and Dronova 2020; McKown et al. 2021; Antonijević et al. 2023). Intra-annual shifts in patch distribution may even occur in some systems (Jeffrey et al. 2019). Patches may interact, meaning that configurational aspects such as patch size, shape, and arrangement can influence processes (Turner 2005). This has been largely unexplored in the context of wetland CH_4 fluxes, but Matthes et al. (2014) found that the fractal dimension of vegetated patches explained variability in fluxes beyond patch composition alone. Finally, vegetation patches may not fully capture the spatial variability of CH_4 drivers (Briones et al. 2022), and the best representation of spatial heterogeneity likely involves a combination of discrete and continuous approaches (Gustafson 1998).

Interdependence of vegetation and environmental influences

We have proposed various biogeochemical mechanisms that may contribute to patch variability in CH_4 fluxes, but we were unable to determine whether vegetation or the environment were the dominant drivers. Distinguishing these sources of variability is an important avenue for future research on, for example, the impacts of non-native plant colonization (Bezabih Beyene et al. 2022) and strategies to minimize CH_4 emissions in restored or created wetlands (Silvey et al. 2019). However, separating vegetation and environmental effects may not always be feasible. The abiotic environment (e.g., hydrology, soil physicochemical properties) controls plant survival and growth, while plants, in turn, modify the environment through processes like transpiration and root exudation (Moor et al. 2017). Further, many plant functional traits reflect both species identity and environmental context (i.e., "response traits"; Engelhardt 2006). For example, root aerenchyma development is a species-specific trait that can affect CH_4 cycling, but its expression depends on flooding and oxygen availability during growth (Smirnoff and Crawford 1983). A reductionist approach may therefore overlook the entanglement of vegetation and environmental influences, and a more nuanced understanding of spatial heterogeneity may be gained by exploring how these factors interact to shape ecosystem processes.

Conclusions

We showed that wetland vegetation patches exhibit distinct CH_4 signals throughout the growing season, likely driven by differences in the mechanisms that regulate fluxes. Our results demonstrate that patch types are important for understanding spatial variability in wetland CH_4 fluxes and support the incorporation of a patch-explicit representation to reduce CH_4 uncertainty in process-based models and inventories (Dinsmore et al. 2009). Amidst global change, accounting for patch variability is essential even when ecosystem-scale flux measurements are available as shifts in vegetation cover are expected to affect greenhouse gas exchange, and certain patch types may respond disproportionately to wetland-scale disturbance (Urbanová et al. 2012; Rietl et al. 2017). Attributing patch-specific CH_4 fluxes could also inform practices to minimize greenhouse gas emissions in managed and restored wetlands (Tak et al. 2023), although these strategies must be balanced with targeted ecosystem services (e.g., nutrient retention; Kasak et al. 2020). In addition to CH_4 flux, other consequential wetland processes may be best represented at the patch scale, and further research should

address the extent to which patches drive spatial heterogeneity in wetland ecosystem processing.

Acknowledgements The authors are grateful to The Nature Conservancy for providing access to the study sites and their stewardship of the land. We recognize Dr. Kelly Hondula's contribution to the early conceptualization of our statistical methods. We thank Dr. Alec Armstrong for his input on study design and data analysis, and for his assistance with field work. We also thank Dr. Christine Maietta and Chloe Kesey for their field assistance. Finally, we are grateful to Drs. Stephanie Yarwood and Andy Baldwin for the flux chambers, and Dr. Greg McCarty for the PhenoCam imagery.

Author contributions Conceptualization: Graham A. Stewart, Margaret A. Palmer; methodology: Graham A. Stewart, Aileen K. Taylor; formal analysis: Graham A. Stewart; investigation: Graham A. Stewart, Sean J. Sharp, Aileen K. Taylor; writing – original draft: Graham A. Stewart; writing—review & editing: Graham A. Stewart, Sean J. Sharp, Aileen K. Taylor, Michael R. Williams, Margaret A. Palmer; funding acquisition: Margaret A. Palmer.

Funding This research was supported by grants to Margaret A. Palmer from the National Science Foundation (DEB-1856200 and DBI-1639145).

Data availability The data and analysis code from this study are openly available at https://doi.org/10.5281/zenodo.12518747.

Declarations

Conflict of interest The authors declare that they have no competing interests.

References

Akhtar H, Lupascu M, Sukri RS et al (2020) Significant sedge-mediated methane emissions from degraded tropical peatlands. Environ Res Lett 16:014002. https://doi.org/10.1088/1748-9326/abc7dc

Andrews SE, Schultz R, Frey SD et al (2013) Plant community structure mediates potential methane production and potential iron reduction in wetland mesocosms. Ecosphere 4:44. https://doi.org/10.1890/ES12-00314.1

Anthony TL, Silver WL (2021) Hot moments drive extreme nitrous oxide and methane emissions from agricultural peatlands. Glob Chang Biol 27:5141–5153. https://doi.org/10.1111/gcb.15802

Antonijević D, Hoffmann M, Prochnow A et al (2023) The unexpected long period of elevated CH_4 emissions from an inundated fen meadow ended only with the occurrence of cattail (Typha latifolia). Glob Chang Biol 29:3678–3691. https://doi.org/10.1111/gcb.16713

Baldocchi DD, Falge E, Gu L et al (2001) FLUXNET: a new tool to study the temporal and spatial variability of ecosystem–scale carbon dioxide, water vapor, and energy flux densities. Bull Am Meteorol Soc 82:2415–2434. https://doi.org/10.1175/1520-0477(2001)082%3c2415:FANTTS%3e2.3.CO;2

Bao T, Jia G, Xu X (2021) Wetland heterogeneity determines methane emissions: a pan-Arctic synthesis. Environ Sci Technol 55:10152–10163. https://doi.org/10.1021/acs.est.1c01616

Barbosa PM, Melack JM, Amaral JHF et al (2021) Large seasonal and habitat differences in methane ebullition on the Amazon floodplain. J Geophys Res Biogeosciences 126:e2020JG005911. https://doi.org/10.1029/2020JG005911

Bastviken D, Treat CC, Pangala SR et al (2023) The importance of plants for methane emission at the ecosystem scale. Aquat Bot 184:103596. https://doi.org/10.1016/j.aquabot.2022.103596

Bates D, Mächler M, Bolker B, Walker S (2015) Fitting linear mixed-effects models using lme4. J Stat Softw 67:1–48. https://doi.org/10.18637/jss.v067.i01

Berg G, Smalla K (2009) Plant species and soil type cooperatively shape the structure and function of microbial communities in the rhizosphere. FEMS Microbiol Ecol 68:1–13. https://doi.org/10.1111/j.1574-6941.2009.00654.x

Bezabih Beyene B, Li J, Yuan J et al (2022) Non-native plant invasion can accelerate global climate change by increasing wetland methane and terrestrial nitrous oxide emissions. Glob Chang Biol 28:5453–5468. https://doi.org/10.1111/gcb.16290

Bhullar GS, Edwards PJ, Olde Venterink H (2013a) Variation in the plant-mediated methane transport and its importance for methane emission from intact wetland peat mesocosms. J Plant Ecol 6:298–304. https://doi.org/10.1093/jpe/rts045

Bhullar GS, Iravani M, Edwards PJ, Olde Venterink H (2013b) Methane transport and emissions from soil as affected by water table and vascular plants. BMC Ecol 13:32. https://doi.org/10.1186/1472-6785-13-32

Bousquet P, Ciais P, Miller JB et al (2006) Contribution of anthropogenic and natural sources to atmospheric methane variability. Nature 443:439–443. https://doi.org/10.1038/nature05132

Bridgham SD, Cadillo-Quiroz H, Keller JK, Zhuang Q (2013) Methane emissions from wetlands: biogeochemical,

microbial, and modeling perspectives from local to global scales. Glob Chang Biol 19:1325–1346. https://doi.org/10.1111/gcb.12131

Briones MJI, Juan-Ovejero R, McNamara NP, Ostle NJ (2022) Microbial "hotspots" of organic matter decomposition in temperate peatlands are driven by local spatial heterogeneity in abiotic conditions and not by vegetation structure. Soil Biol Biochem 165:108501. https://doi.org/10.1016/j.soilbio.2021.108501

Capps KA, Rancatti R, Tomczyk N et al (2014) Biogeochemical hotspots in forested landscapes: the role of vernal pools in denitrification and organic matter processing. Ecosystems 17:1455–1468. https://doi.org/10.1007/s10021-014-9807-z

Caraco N, Cole J, Findlay S, Wigand C (2006) Vascular plants as engineers of oxygen in aquatic systems. Bioscience 56:219–225. https://doi.org/10.1641/0006-3568(2006)056[0219:VPAEOO]2.0.CO;2

Carmichael MJ, Bernhardt ES, Bräuer SL, Smith WK (2014) The role of vegetation in methane flux to the atmosphere: should vegetation be included as a distinct category in the global methane budget? Biogeochemistry 119:1–24. https://doi.org/10.1007/s10533-014-9974-1

Carpenter B, Gelman A, Hoffman MD et al (2017) Stan: a probabilistic programming language. J Stat Softw 76:1–32. https://doi.org/10.18637/jss.v076.i01

Chu H, Luo X, Ouyang Z et al (2021) Representativeness of eddy-covariance flux footprints for areas surrounding AmeriFlux sites. Agric For Meteorol 301–302:108350. https://doi.org/10.1016/j.agrformet.2021.108350

Conn PB, Johnson DS, Williams PJ et al (2018) A guide to Bayesian model checking for ecologists. Ecol Monogr 88:526–542. https://doi.org/10.1002/ecm.1314

Couwenberg J, Thiele A, Tanneberger F et al (2011) Assessing greenhouse gas emissions from peatlands using vegetation as a proxy. Hydrobiologia 674:67–89. https://doi.org/10.1007/s10750-011-0729-x

Davidson SJ, Sloan VL, Phoenix GK et al (2016) Vegetation type dominates the spatial variability in CH_4 emissions across multiple arctic tundra landscapes. Ecosystems 19:1116–1132. https://doi.org/10.1007/s10021-016-9991-0

Day RT, Keddy PA, McNeill J, Carleton T (1988) Fertility and disturbance gradients: a summary model for riverine marsh vegetation. Ecology 69:1044–1054. https://doi.org/10.2307/1941260

De Steven D, Sharitz RR, Singer JH, Barton CD (2006) Testing a passive revegetation approach for restoring coastal plain depression wetlands. Restor Ecol 14:452–460. https://doi.org/10.1111/j.1526-100X.2006.00153.x

Desrosiers K, DelSontro T, del Giorgio PA (2022) Disproportionate contribution of vegetated habitats to the CH_4 and CO_2 budgets of a boreal lake. Ecosystems 25:1522–1541. https://doi.org/10.1007/s10021-021-00730-9

Dinsmore KJ, Skiba UM, Billett MF et al (2009) Spatial and temporal variability in CH_4 and N_2O fluxes from a Scottish ombrotrophic peatland: implications for modelling and up-scaling. Soil Biol Biochem 41:1315–1323. https://doi.org/10.1016/j.soilbio.2009.03.022

Dronova I, Gong P, Wang L (2011) Object-based analysis and change detection of major wetland cover types and their classification uncertainty during the low water period at Poyang Lake, China. Remote Sens Environ 115:3220–3236. https://doi.org/10.1016/j.rse.2011.07.006

Ellison AM (2004) Bayesian inference in ecology. Ecol Lett 7:509–520. https://doi.org/10.1111/j.1461-0248.2004.00603.x

Engelhardt KAM (2006) Relating effect and response traits in submersed aquatic macrophytes. Ecol Appl 16:1808–1820. https://doi.org/10.1890/1051-0761(2006)016[1808:REARTI]2.0.CO;2

Erkkilä K-M, Ojala A, Bastviken D et al (2018) Methane and carbon dioxide fluxes over a lake: comparison between eddy covariance, floating chambers and boundary layer method. Biogeosciences 15:429–445. https://doi.org/10.5194/bg-15-429-2018

Esters L, Rutgersson A, Nilsson E, Sahlée E (2021) Non-local impacts on eddy-covariance air–lake CO_2 fluxes. Bound-Layer Meteorol 178:283–300. https://doi.org/10.1007/s10546-020-00565-2

Eugster W, DelSontro T, Sobek S (2011) Eddy covariance flux measurements confirm extreme CH_4 emissions from a Swiss hydropower reservoir and resolve their short-term variability. Biogeosciences 8:2815–2831. https://doi.org/10.5194/bg-8-2815-2011

Filippa G, Cremonese E, Migliavacca M et al (2016) Phenopix: a R package for image-based vegetation phenology. Agric For Meteorol 220:141–150. https://doi.org/10.1016/j.agrformet.2016.01.006

Finnigan J (2004) The footprint concept in complex terrain. Agric For Meteorol 127:117–129. https://doi.org/10.1016/j.agrformet.2004.07.008

Foken T, Leuning R, Oncley SR et al (2012) Corrections and data quality control. In: Aubinet M, Vesala T, Papale D (eds) Eddy covariance: a practical guide to measurement and data analysis. Springer Netherlands, Dordrecht, pp 85–131

Forbrich I, Kutzbach L, Wille C et al (2011) Cross-evaluation of measurements of peatland methane emissions on microform and ecosystem scales using high-resolution landcover classification and source weight modelling. Agric For Meteorol 151:864–874. https://doi.org/10.1016/j.agrformet.2011.02.006

Ge M, Korrensalo A, Laiho R et al (2023) Plant phenology and species-specific traits control plant CH_4 emissions in a northern boreal fen. New Phytol 238:1019–1032. https://doi.org/10.1111/nph.18798

Girkin NT, Turner BL, Ostle N et al (2018) Root exudate analogues accelerate CO_2 and CH_4 production in tropical peat. Soil Biol Biochem 117:48–55. https://doi.org/10.1016/j.soilbio.2017.11.008

Girkin NT, Vane CH, Cooper HV et al (2019) Spatial variability of organic matter properties determines methane fluxes in a tropical forested peatland. Biogeochemistry 142:231–245. https://doi.org/10.1007/s10533-018-0531-1

Goodrich B, Gabry J, Ali I, Brilleman S (2020) rstanarm: Bayesian applied regression modeling via Stan

Goud EM, Moore TR, Roulet NT (2017) Predicting peatland carbon fluxes from non-destructive plant traits. Funct Ecol 31:1824–1833. https://doi.org/10.1111/1365-2435.12891

Goud EM, Touchette S, Strachan IB, Strack M (2022) Graminoids vary in functional traits, carbon dioxide and methane fluxes in a restored peatland: implications for modelling carbon storage. J Ecol 110:2105–2117. https://doi.org/10.1111/1365-2745.13932

Grasset C, Abril G, Mendonça R et al (2019) The transformation of macrophyte-derived organic matter to methane relates to plant water and nutrient contents. Limnol Oceanogr 64:1737–1749. https://doi.org/10.1002/lno.11148

Gray A, Levy PE, Cooper MDA et al (2013) Methane indicator values for peatlands: a comparison of species and functional groups. Glob Chang Biol 19:1141–1150. https://doi.org/10.1111/gcb.12120

Gustafson EJ (1998) Quantifying landscape spatial pattern: what is the state of the art? Ecosystems 1:143–156. https://doi.org/10.1007/s100219900011

Hammond MP, Kolasa J (2014) Spatial variation as a tool for inferring temporal variation and diagnosing types of mechanisms in ecosystems. PLoS ONE 9:e89245. https://doi.org/10.1371/journal.pone.0089245

Harrison XA, Donaldson L, Correa-Cano ME et al (2018) A brief introduction to mixed effects modelling and multimodel inference in ecology. PeerJ 6:e4794. https://doi.org/10.7717/peerj.4794

Helfter C, Gondwe M, Murray-Hudson M et al (2022) Phenology is the dominant control of methane emissions in a tropical non-forested wetland. Nat Commun 13:133. https://doi.org/10.1038/s41467-021-27786-4

Hersbach H, Bell B, Berrisford P et al (2020) The ERA5 global reanalysis. Q J R Meteorol Soc 146:1999–2049. https://doi.org/10.1002/qj.3803

Holland EA, Robertson GP, Greenberg J et al (1999) Soil CO_2, N_2O, and CH_4 exchange. In: Robertson GP, Bledsoe CS, Coleman DC, Sollins P (eds) Standard soil methods for long-term ecological research. Oxford University Press, New York, pp 185–201

Holm GO, Sasser CE (2008) The management and ecology of the wetland grass, maidencane. J Aquat Plant Manag 46:51–60

Hondula KL, Jones CN, Palmer MA (2021) Effects of seasonal inundation on methane fluxes from forested freshwater wetlands. Environ Res Lett 16:084016. https://doi.org/10.1088/1748-9326/ac1193

Hufkens K, Basler D, Milliman T et al (2018) An integrated phenology modelling framework in R. Methods Ecol Evol 9:1276–1285. https://doi.org/10.1111/2041-210X.12970

Hutjes RWA, Vellinga OS, Gioli B, Miglietta F (2010) Disaggregation of airborne flux measurements using footprint analysis. Agric For Meteorol 150:966–983. https://doi.org/10.1016/j.agrformet.2010.03.004

Jamoneau A, Jan G, Petitcollin T, Ribaudo C (2017) Biomass as a proxy for available surface area in freshwater macrophytes: influence of seasonality. Aquat Bot 142:91–95. https://doi.org/10.1016/j.aquabot.2017.07.005

Jeffrey LC, Maher DT, Johnston SG et al (2019) Wetland methane emissions dominated by plant-mediated fluxes: contrasting emissions pathways and seasons within a shallow freshwater subtropical wetland. Limnol Oceanogr 64:1895–1912. https://doi.org/10.1002/lno.11158

Johns CV, Brownstein G, Fletcher A et al (2015) Detecting the effects of water regime on wetland plant communities: which plant indicator groups perform best? Aquat Bot 123:54–63. https://doi.org/10.1016/j.aquabot.2015.02.002

Jones CG, Lawton JH, Shachak M (1994) Organisms as ecosystem engineers. Oikos 69:373–386. https://doi.org/10.2307/3545850

Kao-Kniffin J, Freyre DS, Balser TC (2010) Methane dynamics across wetland plant species. Aquat Bot 93:107–113. https://doi.org/10.1016/j.aquabot.2010.03.009

Kasak K, Valach AC, Rey-Sanchez C et al (2020) Experimental harvesting of wetland plants to evaluate trade-offs between reducing methane emissions and removing nutrients accumulated to the biomass in constructed wetlands. Sci Total Environ 715:136960. https://doi.org/10.1016/j.scitotenv.2020.136960

Keshta AE, Yarwood SA, Baldwin AH (2023) Methane emissions are highly variable across wetland habitats in natural and restored tidal freshwater wetlands. Wetlands 43:53. https://doi.org/10.1007/s13157-023-01701-7

Kim J, Hwang T, Schaaf CL et al (2018) Seasonal variation of source contributions to eddy-covariance CO_2 measurements in a mixed hardwood-conifer forest. Agric For Meteorol 253–254:71–83. https://doi.org/10.1016/j.agrformet.2018.02.004

Kim Y, Johnson MS, Knox SH et al (2020) Gap-filling approaches for eddy covariance methane fluxes: a comparison of three machine learning algorithms and a traditional method with principal component analysis. Glob Chang Biol 26:1499–1518. https://doi.org/10.1111/gcb.14845

Kljun N, Calanca P, Rotach MW, Schmid HP (2015) A simple two-dimensional parameterisation for Flux Footprint Prediction (FFP). Geosci Model Dev 8:3695–3713. https://doi.org/10.5194/gmd-8-3695-2015

Korrensalo A, Mammarella I, Alekseychik P et al (2022) Plant mediated methane efflux from a boreal peatland complex. Plant Soil 471:375–392. https://doi.org/10.1007/s11104-021-05180-9

Krauss KW, Holm GO, Perez BC et al (2016) Component greenhouse gas fluxes and radiative balance from two deltaic marshes in Louisiana: pairing chamber techniques and eddy covariance. J Geophys Res Biogeosciences 121:1503–1521. https://doi.org/10.1002/2015JG003224

Laanbroek HJ (2010) Methane emission from natural wetlands: interplay between emergent macrophytes and soil microbial processes. A mini-review. Ann Bot 105:141–153. https://doi.org/10.1093/aob/mcp201

Laine AM, Korrensalo A, Tuittila E-S (2022) Plant functional traits play the second fiddle to plant functional types in explaining peatland CO_2 and CH_4 gas exchange. Sci Total Environ 834:155352. https://doi.org/10.1016/j.scitotenv.2022.155352

Lampela M, Jauhiainen J, Kämäri I et al (2016) Ground surface microtopography and vegetation patterns in a tropical peat swamp forest. CATENA 139:127–136. https://doi.org/10.1016/j.catena.2015.12.016

Levy P, Drewer J, Jammet M et al (2020) Inference of spatial heterogeneity in surface fluxes from eddy covariance data: a case study from a subarctic mire ecosystem. Agric

For Meteorol 280:107783. https://doi.org/10.1016/j.agrformet.2019.107783
Määttä T, Malhotra A (2024) The hidden roots of wetland methane emissions. Glob Chang Biol 30:e17127. https://doi.org/10.1111/gcb.17127
Marani M, Silvestri S, Belluco E et al (2006) Spatial organization and ecohydrological interactions in oxygen-limited vegetation ecosystems. Water Resour Res 42:W06D06. https://doi.org/10.1029/2005WR004582
Marton JM, Creed IF, Lewis DB et al (2015) Geographically isolated wetlands are important biogeochemical reactors on the landscape. Bioscience 65:408–418. https://doi.org/10.1093/biosci/biv009
Matthes JH, Sturtevant C, Verfaillie J et al (2014) Parsing the variability in CH_4 flux at a spatially heterogeneous wetland: integrating multiple eddy covariance towers with high-resolution flux footprint analysis. J Geophys Res Biogeosciences 119:1322–1339. https://doi.org/10.1002/2014JG002642
McClain ME, Boyer EW, Dent CL et al (2003) Biogeochemical hot spots and hot moments at the interface of terrestrial and aquatic ecosystems. Ecosystems 6:301–312. https://doi.org/10.1007/s10021-003-0161-9
McEwing KR, Fisher JP, Zona D (2015) Environmental and vegetation controls on the spatial variability of CH_4 emission from wet-sedge and tussock tundra ecosystems in the Arctic. Plant Soil 388:37–52. https://doi.org/10.1007/s11104-014-2377-1
McKown JG, Moore GE, Payne AR et al (2021) Successional dynamics of a 35 year old freshwater mitigation wetland in southeastern New Hampshire. PLoS ONE 16:e0251748. https://doi.org/10.1371/journal.pone.0251748
McNicol G, Sturtevant CS, Knox SH et al (2017) Effects of seasonality, transport pathway, and spatial structure on greenhouse gas fluxes in a restored wetland. Glob Chang Biol 23:2768–2782. https://doi.org/10.1111/gcb.13580
McNicol G, Fluet-Chouinard E, Ouyang Z et al (2023) Upscaling wetland methane emissions from the FLUXNET-CH4 eddy covariance network (UpCH4 v1.0): model development, network assessment, and budget comparison. AGU Adv 4:e2023AV000956. https://doi.org/10.1029/2023AV000956
Moncrieff J, Clement R, Finnigan J, Meyers T (2004) Averaging, detrending, and filtering of eddy covariance time series. In: Lee X, Massman W, Law B (eds) Handbook of micrometeorology. Springer, Dordrecht, pp 7–31
Moncrieff JB, Massheder JM, de Bruin H et al (1997) A system to measure surface fluxes of momentum, sensible heat, water vapour and carbon dioxide. J Hydrol 188–189:589–611. https://doi.org/10.1016/S0022-1694(96)03194-0
Moor H, Rydin H, Hylander K et al (2017) Towards a trait-based ecology of wetland vegetation. J Ecol 105:1623–1635. https://doi.org/10.1111/1365-2745.12734
Morin TH, Bohrer G, Stefanik KC et al (2017) Combining eddy-covariance and chamber measurements to determine the methane budget from a small, heterogeneous urban floodplain wetland park. Agric For Meteorol 237–238:160–170. https://doi.org/10.1016/j.agrformet.2017.01.022
Nahlik AM, Mitsch WJ (2011) Methane emissions from tropical freshwater wetlands located in different climatic zones of Costa Rica. Glob Chang Biol 17:1321–1334. https://doi.org/10.1111/j.1365-2486.2010.02190.x
Neftel A, Spirig C, Ammann C (2008) Application and test of a simple tool for operational footprint evaluations. Environ Pollut 152:644–652. https://doi.org/10.1016/j.envpol.2007.06.062
Noyce GL, Megonigal JP (2021) Biogeochemical and plant trait mechanisms drive enhanced methane emissions in response to whole-ecosystem warming. Biogeosciences 18:2449–2463. https://doi.org/10.5194/bg-18-2449-2021
Ogle K, Barber JJ (2020) Ensuring identifiability in hierarchical mixed effects Bayesian models. Ecol Appl 30:e02159. https://doi.org/10.1002/eap.2159
Palozzi JE, Lindo Z (2017) Boreal peat properties link to plant functional traits of ecosystem engineers. Plant Soil 418:277–291. https://doi.org/10.1007/s11104-017-3291-0
Pan Y, Cieraad E, Clarkson BR et al (2020) Drivers of plant traits that allow survival in wetlands. Funct Ecol 34:956–967. https://doi.org/10.1111/1365-2435.13541
Pesaran MH, Smith RP (2019) A Bayesian analysis of linear regression models with highly collinear regressors. Econom Stat 11:1–21. https://doi.org/10.1016/j.ecosta.2018.10.001
Phillips PJ, Shedlock RJ (1993) Hydrology and chemistry of groundwater and seasonal ponds in the Atlantic Coastal Plain in Delaware, USA. J Hydrol 141:157–178. https://doi.org/10.1016/0022-1694(93)90048-E
Praetzel LSE, Schmiedeskamp M, Knorr K-H (2021) Temperature and sediment properties drive spatiotemporal variability of methane ebullition in a small and shallow temperate lake. Limnol Oceanogr 66:2598–2610. https://doi.org/10.1002/lno.11775
Repo E, Huttunen JT, Naumov AV et al (2007) Release of CO_2 and CH_4 from small wetland lakes in western Siberia. Tellus B Chem Phys Meteorol 59:788–796. https://doi.org/10.1111/j.1600-0889.2007.00301.x
Rey-Sanchez AC, Morin TH, Stefanik KC et al (2018) Determining total emissions and environmental drivers of methane flux in a Lake Erie estuarine marsh. Ecol Eng 114:7–15. https://doi.org/10.1016/j.ecoleng.2017.06.042
Richardson AD, Hufkens K, Milliman T et al (2018) Tracking vegetation phenology across diverse North American biomes using PhenoCam imagery. Sci Data 5:180028. https://doi.org/10.1038/sdata.2018.28
Rietl AJ, Nyman JA, Lindau CW, Jackson CR (2017) Wetland methane emissions altered by vegetation disturbance: an interaction between stem clipping and nutrient enrichment. Aquat Bot 136:205–211. https://doi.org/10.1016/j.aquabot.2016.10.008
Schmid HP (1997) Experimental design for flux measurements: matching scales of observations and fluxes. Agric For Meteorol 87:179–200. https://doi.org/10.1016/S0168-1923(97)00011-7
Schneider CA, Rasband WS, Eliceiri KW (2012) NIH Image to ImageJ: 25 years of image analysis. Nat Methods 9:671–675. https://doi.org/10.1038/nmeth.2089
Schultz RE, Pett L (2018) Plant community effects on CH_4 fluxes, root surface area, and carbon storage in

experimental wetlands. Ecol Eng 114:96–103. https://doi.org/10.1016/j.ecoleng.2017.06.027

Sharp SJ, Maietta CE, Stewart GA et al (2024) Net methane production predicted by patch characteristics in a freshwater wetland. J Geophys Res Biogeosciences 129:e2023JG007814. https://doi.org/10.1029/2023JG007814

Silvey C, Jarecke KM, Hopfensperger K et al (2019) Plant species and hydrology as controls on constructed wetland methane fluxes. Soil Sci Soc Am J 83:848–855. https://doi.org/10.2136/sssaj2018.11.0421

Smirnoff N, Crawford RMM (1983) Variation in the structure and response to flooding of root aerenchyma in some wetland plants. Ann Bot 51:237–249

Spadafora E, Leslie AW, Culler LE et al (2016) Macroinvertebrate community convergence between natural, rehabilitated, and created wetlands. Restor Ecol 24:463–470. https://doi.org/10.1111/rec.12352

Stoy PC, Cook AA, Dore JE et al (2021) Methane efflux from an American bison herd. Biogeosciences 18:961–975. https://doi.org/10.5194/bg-18-961-2021

Ström L, Mastepanov M, Christensen TR (2005) Species-specific effects of vascular plants on carbon turnover and methane emissions from wetlands. Biogeochemistry 75:65–82. https://doi.org/10.1007/s10533-004-6124-1

Sutton-Grier AE, Megonigal JP (2011) Plant species traits regulate methane production in freshwater wetland soils. Soil Biol Biochem 43:413–420. https://doi.org/10.1016/j.soilbio.2010.11.009

Taddeo S, Dronova I (2020) Landscape metrics of post-restoration vegetation dynamics in wetland ecosystems. Landsc Ecol 35:275–292. https://doi.org/10.1007/s10980-019-00946-0

Tak DBY, Vroom RJE, Lexmond R et al (2023) Water level and vegetation type control carbon fluxes in a newly-constructed soft-sediment wetland. Wetl Ecol Manag 31:583–594. https://doi.org/10.1007/s11273-023-09936-1

Teh YA, Silver WL, Sonnentag O et al (2011) Large greenhouse gas emissions from a temperate peatland pasture. Ecosystems 14:311–325. https://doi.org/10.1007/s10021-011-9411-4

Theus ME, Ray NE, Bansal S, Holgerson MA (2023) Submersed macrophyte density regulates aquatic greenhouse gas emissions. J Geophys Res Biogeosciences 128:e2023JG007758. https://doi.org/10.1029/2023JG007758

Turetsky MR, Kotowska A, Bubier J et al (2014) A synthesis of methane emissions from 71 northern, temperate, and subtropical wetlands. Glob Chang Biol 20:2183–2197. https://doi.org/10.1111/gcb.12580

Turner MG (2005) Landscape ecology: what is the state of the science? Annu Rev Ecol Evol Syst 36:319–344. https://doi.org/10.1146/annurev.ecolsys.36.102003.152614

Turner JC, Moorberg CJ, Wong A et al (2020) Getting to the root of plant-mediated methane emissions and oxidation in a thermokarst bog. J Geophys Res Biogeosciences 125:e2020JG005825. https://doi.org/10.1029/2020JG005825

Urbanová Z, Picek T, Hájek T et al (2012) Vegetation and carbon gas dynamics under a changed hydrological regime in central European peatlands. Plant Ecol Divers 5:89–103. https://doi.org/10.1080/17550874.2012.688069

van den Berg M, van den Elzen E, Ingwersen J et al (2020) Contribution of plant-induced pressurized flow to CH_4 emission from a Phragmites fen. Sci Rep 10:12304. https://doi.org/10.1038/s41598-020-69034-7

Vázquez-Lule A, Vargas R (2021) Biophysical drivers of net ecosystem and methane exchange across phenological phases in a tidal salt marsh. Agric For Meteorol 300:108309. https://doi.org/10.1016/j.agrformet.2020.108309

Vickers D, Mahrt L (1997) Quality control and flux sampling problems for tower and aircraft data. J Atmospheric Ocean Technol 14:512–526. https://doi.org/10.1175/1520-0426(1997)014%3c0512:QCAFSP%3e2.0.CO;2

Villa JA, Ju Y, Stephen T et al (2020) Plant-mediated methane transport in emergent and floating-leaved species of a temperate freshwater mineral-soil wetland. Limnol Oceanogr 65:1635–1650. https://doi.org/10.1002/lno.11467

Villa JA, Ju Y, Yazbeck T et al (2021) Ebullition dominates methane fluxes from the water surface across different ecohydrological patches in a temperate freshwater marsh at the end of the growing season. Sci Total Environ 767:144498. https://doi.org/10.1016/j.scitotenv.2020.144498

Vroom RJE, van den Berg M, Pangala SR et al (2022) Physiological processes affecting methane transport by wetland vegetation—a review. Aquat Bot 182:103547. https://doi.org/10.1016/j.aquabot.2022.103547

Waldo NB, Hunt BK, Fadely EC et al (2019) Plant root exudates increase methane emissions through direct and indirect pathways. Biogeochemistry 145:213–234. https://doi.org/10.1007/s10533-019-00600-6

Waldo NB, Chistoserdova L, Hu D et al (2022) Impacts of the wetland sedge Carex aquatilis on microbial community and methane metabolisms. Plant Soil 471:491–506. https://doi.org/10.1007/s11104-021-05239-7

Webb EK, Pearman GI, Leuning R (1980) Correction of flux measurements for density effects due to heat and water vapour transfer. Q J R Meteorol Soc 106:85–100. https://doi.org/10.1002/qj.49710644707

Whitaker J, Richardson HR, Ostle NJ et al (2021) Plant functional type indirectly affects peatland carbon fluxes and their sensitivity to environmental change. Eur J Soil Sci 72:1042–1053. https://doi.org/10.1111/ejss.13048

Whiting GJ, Chanton JP (1993) Primary production control of methane emission from wetlands. Nature 364:794–795. https://doi.org/10.1038/364794a0

Whiting GJ, Chanton JP (2001) Greenhouse carbon balance of wetlands: methane emission versus carbon sequestration. Tellus B Chem Phys Meteorol 53:521–528. https://doi.org/10.3402/tellusb.v53i5.16628

Wilczak JM, Oncley SP, Stage SA (2001) Sonic anemometer tilt correction algorithms. Bound-Layer Meteorol 99:127–150. https://doi.org/10.1023/A:1018966204465

Williams AS, Mushet DM, Lang M et al (2020) Improving the ability to include freshwater wetland plants in process-based models. J Soil Water Conserv 75:704–712. https://doi.org/10.2489/jswc.2020.00089

Yavitt JB, Burtis JC, Smemo KA, Welsch M (2018) Plot-scale spatial variability of methane, respiration, and net nitrogen mineralization in muck-soil wetlands across a land use gradient. Geoderma 315:11–19. https://doi.org/10.1016/j.geoderma.2017.11.038

Yoshida N, Iguchi H, Yurimoto H et al (2014) Aquatic plant surface as a niche for methanotrophs. Front Microbiol 5:30. https://doi.org/10.3389/fmicb.2014.00030